Chiral corrections to hyperon axial form factors

Fu-Jiun Jiang[1,*] and B. C. Tiburzi[2,3,+]

[1]Institute for Theoretical Physics, Bern University, Sidlerstrasse 5, CH-3012 Bern, Switzerland
[2]Department of Physics, Duke University, Box 90305, Durham, North Carolina 27708-0305, USA
[3]Maryland Center for Fundamental Physics, Department of Physics, University of Maryland, College Park, Maryland 20742-4111, USA

(Received 26 January 2008; published 20 May 2008)

We study the complete set of flavor-changing hyperon axial-current matrix elements at small momentum transfer. Using partially quenched heavy baryon chiral perturbation theory, we derive the chiral and momentum behavior of the axial and induced pseudoscalar form factors. The meson pole contributions to the latter posses a striking signal for chiral physics. We argue that the study of hyperon axial matrix elements enables a systematic lattice investigation of the efficacy of three-flavor chiral expansions in the baryon sector. This can be achieved by considering chiral corrections to $SU(3)$ symmetry predictions, and their partially quenched generalizations. In particular, despite the presence of eight unknown low-energy constants, we are able to make next-to-leading order symmetry breaking predictions for two linear combinations of axial charges.

DOI: 10.1103/PhysRevD.77.094506 PACS numbers: 12.38.Gc, 12.39.Fe

I. INTRODUCTION

For the last decade, lattice gauge theory techniques have made dramatic progress in increasing our understanding of the nonperturbative regime of QCD [1]. Despite considerable advances, there are still sources of systematic error in lattice data, for example, the finite extent of the lattice and the unphysically large quark masses. Fortunately low-energy hadron properties are dominated by virtual pion interactions, and the systematic treatment of such interactions using chiral perturbation theory (χPT) allows one to parametrize the lattice volume and quark mass dependence of certain observables. There has been considerable activity to understand theoretically the quark mass and lattice volume dependence of hadronic observables. Further extensions of chiral perturbation theory have been developed to account for quenching and partially quenching [2–5], and discretization errors [6,7]. An example is the nucleon axial charge, g_A. Recent lattice studies have made impressive strides toward determining g_A [8,9]. In tandem, recent χPT analyses of the chiral [10–12], continuum [13,14], and volume extrapolations [15–17] are poised to connect the data to the physical point. We are beginning to enter a stage in which the combination of lattice QCD data and χPT will enable the study the hadronic properties from the first principles.

A serious issue, however, confronts this program when extended to hyperon observables. Various $SU(3)$ predictions for hyperon properties compare poorly to experiment in contrast to the many successful $SU(2)$ predictions for the nucleon. While χPT can be used to systematically incorporate effects from the strange quark mass, the systematic expansion in the baryon sector has terms that scale (in the worst case) as $\sim m_\eta/M$, where m_η is the mass of the η-meson and M is the average hyperon mass. A well-known conflict between χPT analyses and experimental data exist for hyperon decays. For example, the nonleptonic weak decays, $\Lambda \to p\pi^-$ and $\Sigma^+ \to n\pi^+$, have been extensively investigated experimentally. In particular the s- and p-wave contributions to these weak decays are determined to high precision. Although efforts in the framework of χPT have been devoted to understanding these nonleptonic decays theoretically [18–27], long-standing disagreement between these theoretical analyses and experimental data remain [28–30].

One is thus led to question the efficacy of three-flavor χPT in the baryon sector. Without this systematic model-independent expansion, lattice QCD data for hyperon properties cannot be reliably extrapolated to the physical values of the quark masses. Additionally volume and continuum extrapolations using three-flavor χPT cannot be trusted. Indeed the first lattice calculation of hyperon axial charges, $g_{\Sigma\Sigma}$ and $g_{\Xi\Xi}$ [31,32], shows little evidence for the one-loop predictions from (partially quenched) χPT [33]. The lattice, however, can provide a diagnostic tool to investigate the condition of three-flavor χPT. A complete study of baryon axial charges is the natural starting point. These couplings enter in the loop graphs that determine the long-range chiral corrections to all baryon observables. Input of these measured parameters into χPT expressions allows one to numerically assess the behavior of the long-range contributions in the chiral expansion. This information can then be used to address the convergence of the chiral expansion. Perhaps the expansion is converging to the wrong answer, or perhaps the expansion is not converging at all. If it is the latter case, one can use the lattice to investigate the cause. Perhaps certain observables are cor-

*fjjiang@itp.unibe.ch
+bctiburz@umd.edu

rupted by large values of local contributions that can be isolated and determined from lattice data, or perhaps nearby resonances are leading to large enhancements.

In this work, we provide a follow-up to [33] by determining the full set of hyperon matrix elements of flavor-changing axial currents. We work to next-to-leading order in partially quenched heavy baryon chiral perturbation theory to address both the chiral behavior and momentum-transfer dependence of the axial form factors. Because of meson pole contributions, the pseudoscalar form factor provides an observable well suited for the investigation of chiral physics in three-flavor theories. Despite the accumulation of a large number (eight) of undetermined low-energy constants, we utilize the full set of axial charges to make nontrivial next-to-leading order predictions.

Our paper is organized as follows. First in Sec. II, aspects of PQχPT relevant to our calculations are reviewed. In Sec. III, we map the PQQCD axial-vector current onto operators in PQχPT up to next-to-leading order. The hyperon axial-current matrix elements are determined for $|\Delta I| = 1$ transitions (Sec. III B), and $|\Delta S| = 1$ transitions (Sec. III C). Various wave function renormalization factors are collected in the appendix. Nontrivial next-to-leading order predictions for axial charges, and a discussion of $SU(3)$ breaking corrections are presented in Sec. IV, which concludes our paper.

II. PARTIALLY QUENCHED CHIRAL LAGRANGIAN

Before we detail the calculation of the axial-current matrix elements, we briefly review partially quenched chiral perturbation theory. We recall the partially quenched chiral Lagrangian in the meson sector first and emphasize the relation between lattice measured meson masses and the parameters of the Lagrangian. The baryon Lagrangian is then described in detail.

A. Mesons

The lattice action we consider here is comprised of valence and sea quarks, each of which comes in three flavors. In the continuum limit, this action can be described by the partially quenched QCD (PQQCD) Lagrange density, which is given by

$$\mathcal{L} = \bar{Q} i \not{D} Q - \bar{Q} m_Q Q, \tag{1}$$

where the quark fields appear in the vector Q, which has entries

$$Q = (u, d, s, j, l, r, \tilde{u}, \tilde{d}, \tilde{s})^T, \tag{2}$$

and transforms in the fundamental representation of the graded group $SU(6|3)$. The quark components of the field Q satisfy the following graded equal-time commutation relation

$$Q_i^\alpha(\mathbf{x}) Q_k^{\beta\dagger}(\mathbf{y}) - (-)^{\eta_i \eta_k} Q_k^{\beta\dagger}(\mathbf{y}) Q_i^\alpha(\mathbf{x}) = \delta^{\alpha\beta}\delta_{ik}\delta^3(\mathbf{x}-\mathbf{y}), \tag{3}$$

where (α, β) and (i, k) are spin and flavor indices, respectively. The η_k's appearing above are given by $\eta_k = +1$ for $k = 1$–6 and $\eta_k = 0$ for $k = 7$–9. The η_k maintain the graded structure of the Lie algebra. Further, the graded equal-time commutation relations for two Q's or two $Q^\dagger$'s vanish. The partially quenched generalization of the mass matrix m_Q is given by

$$m_Q = \mathrm{diag}(m_u, m_d, m_s, m_j, m_l, m_s, m_u, m_d, m_s). \tag{4}$$

In this work, we enforce the isospin limit in both the valence and sea sectors so that we have

$$m_Q = \mathrm{diag}(\bar{m}, \bar{m}, m_s, m_j, m_j, m_s, \bar{m}, \bar{m}, m_s). \tag{5}$$

Notice that with Eq. (4) [and similarly Eq. (5)], there is an exact cancellation between valence and ghost quark contributions to the determinant in the path integral for the QCD partition function. This cancellation leaves only the contribution from the sea sector. When $m_Q = 0$, the Lagrangian Eq. (1) has a graded $U(6|3)_L \otimes U(6|3)_R$ symmetry which will reduce to $SU(6|3)_L \otimes SU(6|3)_R \otimes U(1)_V$ by the axial anomaly [5]. We assume that the chiral symmetry is spontaneously broken: $SU(6|3)_L \otimes SU(6|3)_R \to SU(6|3)_V$, hence an identification between PQQCD and QCD can be made. The low-energy effective theory of PQQCD is written in terms of the pseudo-Goldstone mesons emerging from spontaneous chiral symmetry breaking. At leading order in an expansion in momentum and quark mass,[1] the PQχPT Lagrangian for the mesons is given by

$$\mathcal{L} = \frac{f^2}{8}\mathrm{str}(\partial^\mu \Sigma^\dagger \partial_\mu \Sigma) + \lambda \mathrm{str}(m_q \Sigma^\dagger + m_q^\dagger \Sigma) - m_0^2 \Phi_0^2, \tag{6}$$

where $f = 132$ MeV, the str( ) denotes a graded flavor trace, and the meson fields are incorporated in Σ through

$$\Sigma = \exp\left(\frac{2i\Phi}{f}\right) = \xi^2, \qquad \Phi = \begin{pmatrix} M & \chi^\dagger \\ \chi & \tilde{M} \end{pmatrix}. \tag{7}$$

The matrices M, $\tilde{M}$ in Eq. (7) contain bosonic mesons, while χ and $\chi^\dagger$ are matrices consisting of fermionic mesons. Here $\Phi_0 = \mathrm{str}(\Phi)/\sqrt{6}$ is the flavor singlet field and is included as a device to obtain the flavor neutral propagators in PQχPT. Expanding the Lagrangian in Eq. (6), one can determine the meson masses which enter into the calculations of baryon observables. In particular, the masses of mesons at leading order with quark content $Q_i \bar{Q}_j'$ are

[1] Here we adopt the standard power counting: $\partial^2 \sim m_q \sim \varepsilon^2$, where ε is a small parameter.

$$m^2_{Q_iQ'_j} = \frac{4\lambda}{f^2}((m_Q)_{ii} + (m_{Q'})_{jj}). \tag{8}$$

The flavor singlet field additionally acquires a mass m_0^2. Because of the strong $U(1)_A$ anomaly, this mass can be taken on the order of the chiral symmetry breaking scale, $m_0 \sim \Lambda_\chi \approx 4\pi f$. The flavor singlet field can thus be integrated out. However, the propagator of the flavor neutral fields deviate from a simple pole form [5]. For a, $b = u$, d, s, the $\eta_a\eta_b$ propagator at leading order is given by [5]

$$\mathcal{G}_{\eta_a\eta_b} = \frac{i\delta^{ab}}{q^2 - m_{aa}^2 + i\epsilon} - \frac{i}{3} \times \frac{(q^2 - m_{jj}^2 + i\epsilon)(q^2 - m_{rr}^2 + i\epsilon)}{(q^2 - m_{aa}^2 + i\epsilon)(q^2 - m_{bb}^2 + i\epsilon)(q^2 - m_X^2 + i\epsilon)}, \tag{9}$$

where the masses of valence-valence mesons m_{aa}^2, m_{bb}^2 and the masses of the sea-sea mesons m_{jj}^2, m_{rr}^2 are given by Eq. (8). In Eq. (9), the mass m_X is defined as $m_X^2 = \frac{1}{3} \times (m_{jj}^2 + 2m_{rr}^2)$. The flavor neutral propagator Eq. (9) can be conveniently written in the form

$$\mathcal{G}_{\eta_a\eta_b} = \delta^{ab} P_a + \mathcal{H}_{aa}(P_a, P_b, P_X), \tag{10}$$

with

$$\begin{aligned}
P_a &= \frac{i}{q^2 - m_{aa}^2 + i\epsilon}, \\
P_b &= \frac{i}{q^2 - m_{bb}^2 + i\epsilon}, \\
P_X &= \frac{i}{q^2 - m_X^2 + i\epsilon}, \\
\mathcal{H}_{ab}(A, B, C) &= -\frac{1}{3}\Bigg[\frac{(m_{jj}^2 - m_{aa}^2)(m_{rr}^2 - m_{aa}^2)}{(m_{aa}^2 - m_{bb}^2)(m_{aa}^2 - m_X^2)} A \\
&\quad - \frac{(m_{jj}^2 - m_{bb}^2)(m_{rr}^2 - m_{bb}^2)}{(m_{aa}^2 - m_{bb}^2)(m_{bb}^2 - m_X^2)} B \\
&\quad + \frac{(m_X^2 - m_{jj}^2)(m_X^2 - m_{rr}^2)}{(m_X^2 - m_{aa}^2)(m_X^2 - m_{bb}^2)} C\Bigg].
\end{aligned} \tag{11}$$

The above form is convenient for contributions from flavor neutral mixing. When there is no mixing, i.e. $a = b$ and $A = B$, the hairpin propagator has a double pole and the limit of Eq. (11) must be taken and produces

$$\begin{aligned}
\mathcal{H}_{aa}(A, A, C) &= -\frac{1}{3}\Bigg[\frac{\partial}{\partial m_{aa}^2} \frac{(m_{jj}^2 - m_{aa}^2)(m_{rr}^2 - m_{aa}^2)}{(m_{aa}^2 - m_X^2)} A \\
&\quad + \frac{(m_{jj}^2 - m_X^2)(m_{rr}^2 - m_X^2)}{(m_X^2 - m_{aa}^2)^2} C\Bigg].
\end{aligned} \tag{12}$$

In partially quenched simulations, one numerically determines the values of the valence pion $m_{\pi,\mathrm{val}}$ and valence kaon $m_{K,\mathrm{val}}$ masses, as well as the sea pion $m_{\pi,\mathrm{sea}}$ and sea kaon $m_{K,\mathrm{sea}}$ masses. When one uses PQχPT to calculate the meson mass dependence of observables, they are expressed in terms of meson masses via the tree-level relation in Eq. (8). To use the lattice determined meson masses in the valence and sea sectors, it is straightforward algebra to convert the loop meson masses appearing in PQχPT to those measured directly on the lattice. Explicitly we have

$$\begin{aligned}
m_{uu}^2 &= m_{\eta_u}^2 = m_{\pi,\mathrm{val}}^2, \\
m_{us}^2 &= m_{K,\mathrm{val}}^2, \\
m_{ss}^2 &= m_{\eta_s}^2 = 2m_{K,\mathrm{val}}^2 - m_{\pi,\mathrm{val}}^2, \\
m_{uj}^2 &= \tfrac{1}{2}(m_{\pi,\mathrm{val}}^2 + m_{\pi,\mathrm{sea}}^2), \\
m_{ur}^2 &= \tfrac{1}{2}(m_{\pi,\mathrm{val}}^2 - m_{\pi,\mathrm{sea}}^2) + m_{K,\mathrm{sea}}^2, \\
m_{sj}^2 &= \tfrac{1}{2}(m_{\pi,\mathrm{sea}}^2 - m_{\pi,\mathrm{val}}^2) + m_{K,\mathrm{val}}^2, \\
m_{sr}^2 &= -\tfrac{1}{2}(m_{\pi,\mathrm{val}}^2 + m_{\pi,\mathrm{sea}}^2) + m_{K,\mathrm{val}}^2 + m_{K,\mathrm{sea}}^2, \\
m_{jj}^2 &= m_{\pi,\mathrm{sea}}^2, \\
m_{rr}^2 &= 2m_{K,\mathrm{sea}}^2 - m_{\pi,\mathrm{sea}}^2, \\
m_X^2 &= \tfrac{4}{3}m_{K,\mathrm{sea}}^2 - \tfrac{1}{3}m_{\pi,\mathrm{sea}}^2.
\end{aligned} \tag{13}$$

These relations must be modified if the source of partial quenching is due to mixed lattice actions, see [34–36].

B. Baryon

In this section, we discuss the baryon sector of PQχPT in the framework of [37–39]. Building blocks for the baryon Lagrangian are the supermultiplets $\mathcal{B}_{ijk}$ and $\mathcal{T}^\mu_{ijk}$. The **240**-dimensional supermultiplet of spin-$\frac{1}{2}$ baryons $\mathcal{B}_{ijk}$ satisfies the following relations under the interchange of the flavor indices [37]:

$$\begin{aligned}
&\mathcal{B}_{ijk} = (-)^{1+\eta_j\eta_k}\mathcal{B}_{ikj}, \\
&\mathcal{B}_{ijk} + (-)^{1+\eta_i\eta_j}\mathcal{B}_{jik} + (-)^{1+\eta_i\eta_j+\eta_j\eta_k+\eta_k\eta_i}\mathcal{B}_{kji} = 0,
\end{aligned} \tag{14}$$

and the familiar octet baryons are embeded in $\mathcal{B}_{ijk}$ through [38,39]

$$\mathcal{B}_{ijk} = \frac{1}{\sqrt{6}}(\epsilon_{ijl}B_k^l + \epsilon_{ikl}B_j^l), \tag{15}$$

where B is the octet baryon matrix

$$B = \begin{pmatrix} \frac{1}{\sqrt{6}}\Lambda + \frac{1}{\sqrt{2}}\Sigma^0 & \Sigma^+ & p \\ \Sigma^- & \frac{1}{\sqrt{6}}\Lambda - \frac{1}{\sqrt{2}}\Sigma^0 & n \\ \Xi^- & \Xi^0 & -\frac{2}{\sqrt{6}}\Lambda \end{pmatrix}. \tag{16}$$

The spin-$\frac{3}{2}$ resonances are contained in the **138**-dimensional supermultiplet $\mathcal{T}_{ijk}$, which satisfies

$$\mathcal{T}_{ijk} = (-)^{1+\eta_i\eta_j}\mathcal{T}_{jik} = (-)^{1+\eta_j\eta_k}\mathcal{T}_{ikj}, \tag{17}$$

under the interchange of flavor indices [37]. Furthermore, one embeds the decuplet baryons in $\mathcal{T}_{ijk}$ by

$$\mathcal{T}_{ijk} = T_{ijk}, \tag{18}$$

where T is a totally symmetric tensor containing the decuplet resonances

$$\begin{aligned} &T_{111} = \Delta^{++}, \qquad T_{112} = \frac{1}{\sqrt{3}}\Delta^{+}, \qquad T_{122} = \frac{1}{\sqrt{3}}\Delta^{0}, \\ &T_{222} = \Delta^{-}, \qquad T_{113} = \frac{1}{\sqrt{3}}\Sigma^{*,+}, \qquad T_{123} = \frac{1}{\sqrt{6}}\Sigma^{*,0}, \\ &T_{223} = \frac{1}{\sqrt{3}}\Sigma^{*,-}, \qquad T_{133} = \frac{1}{\sqrt{3}}\Xi^{*,0}, \\ &T_{233} = \frac{1}{\sqrt{3}}\Xi^{*,-}, \qquad T_{333} = \Omega^{-}. \end{aligned} \tag{19}$$

The free Lagrangian for the **240**-dimensional supermultiplet $\mathcal{B}_{ijk}$ and the **138**-dimensional supermultiplet $\mathcal{T}_{ijk}$ fields in $SU(6|3)$ PQχPT is given by [39]

$$\begin{aligned} \mathcal{L} = {} & i(\bar{\mathcal{B}} v \cdot \mathcal{D}\mathcal{B}) + 2\alpha_M(\bar{\mathcal{B}}\mathcal{B}\mathcal{M}_+) + 2\beta_M(\bar{\mathcal{B}}\mathcal{M}_+\mathcal{B}) \\ & + 2\sigma_M(\bar{\mathcal{B}}\mathcal{B})\mathrm{str}(\mathcal{M}_+) - i(\bar{\mathcal{T}}^\mu v\cdot\mathcal{D}\mathcal{T}_\mu) \\ & + \Delta(\bar{\mathcal{T}}^\mu\mathcal{T}_\mu) + 2\gamma_M(\bar{\mathcal{T}}^\mu\mathcal{M}_+\mathcal{T}_\mu) \\ & - 2\bar{\sigma}_M(\bar{\mathcal{T}}^\mu\mathcal{T}_\mu)\mathrm{str}(\mathcal{M}_+), \end{aligned} \tag{20}$$

where the mass operator $\mathcal{M}_+$ is defined by

$$\mathcal{M}_+ = \tfrac{1}{2}(\xi^\dagger m_Q \xi^\dagger + \xi m_Q \xi). \tag{21}$$

The parameter Δ is the mass splitting between the octet and decuplet baryons in the chiral limit. Phenomenologically we know $\Delta \sim m_\phi$, where ϕ is a $SU(3)$ meson, hence the decuplet baryons must be included as dynamical fields in Eq. (20). The parenthesis notation for flavor contractions used in Eq. (20) is that of [39]. The partially quenched Lagrangian describing the interactions of the $\mathcal{B}_{ijk}$ and $\mathcal{T}^\mu_{ijk}$ with the pseudo-Goldstone mesons is given by [39]

$$\begin{aligned} \mathcal{L} = {} & 2\alpha(\bar{\mathcal{B}}S^\mu\mathcal{B}A_\mu) + 2\beta(\bar{\mathcal{B}}S^\mu A_\mu\mathcal{B}) \\ & + 2\mathcal{H}(\bar{\mathcal{T}}^\nu S^\mu A_\mu \mathcal{T}_\nu) + \sqrt{\frac{3}{2}}\mathcal{C}[(\bar{\mathcal{T}}^\nu A_\nu\mathcal{B}) \\ & + (\bar{\mathcal{B}}A_\nu\mathcal{T}^\nu)]. \end{aligned} \tag{22}$$

The axial-vector and vector meson fields A_μ and V_μ are defined by $A_\mu = \frac{i}{2}(\xi\partial_\mu\xi^\dagger - \xi^\dagger\partial_\mu\xi)$ and $V_\mu = \frac{1}{2}\times(\xi\partial_\mu\xi^\dagger + \xi^\dagger\partial_\mu\xi)$. The latter appears in Eq. (20) for the covariant derivatives of $\mathcal{B}_{ijk}$ and $\mathcal{T}_{ijk}$ that both have the form

$$\begin{aligned} (\mathcal{D}^\mu\mathcal{B})_{ijk} = {} & \partial^\mu\mathcal{B}_{ijk} + (V^\mu)_i^l\mathcal{B}_{ljk} + (-)^{\eta_i(\eta_j+\eta_m)} \\ & \times (V^\mu)_j^m\mathcal{B}_{imk} + (-)^{(\eta_i+\eta_j)(\eta_k+\eta_n)}(V^\mu)_k^n\mathcal{B}_{ijn}. \end{aligned} \tag{23}$$

The vector S_μ is the covariant spin operator [18,19]. The parameters that appear in the PQχPT Lagrangian can be related to those in χPT by matching. To be more specific, one restricts to the $q_{\mathrm{sea}}q_{\mathrm{sea}}q_{\mathrm{sea}}$ sector and compares the PQχPT Lagrangian obtained with that of χPT. With this matching procedure, one finds that $\alpha = \frac{2}{3}D + 2F$, $\beta = -\frac{5}{3}D + F$, and the other parameters $\mathcal{C}$ and $\mathcal{H}$ appearing above have the same numerical values as in χPT [39].

III. THE AXIAL-VECTOR CURRENT

A. The axial-vector current in PQχPT

The baryon matrix elements of the axial-vector current, $j^a_{\mu,5} = \bar{q}\lambda^a\gamma_\mu\gamma_5 q$, have been studied extensively both on the lattice [8,9] and χPT [10–12,15,16,18,19,33,40–46]. In PQQCD, the axial current is defined by $J^a_{\mu,5} = \bar{Q}\bar{\lambda}^a\gamma_\mu\gamma_5 Q$. In general, one must worry that the choice of supermatrices $\bar{\lambda}^a$ is not unique even after the requirement $\mathrm{str}(\bar{\lambda}^a) = 0$ has been enforced. To be relevant for any practical lattice calculation, the choice of PQQCD matrices should maintain the cancellation of valence and ghost quark loops with an operator insertion [33,47]. This is because otherwise the PQQCD theory corresponds to a lattice theory where twice the number of disconnected contractions must be calculated. However, since we are only interested in flavor-changing operators, the self contractions of these operators automatically vanish. Thus we can decouple the ghost and sea quark sectors from the flavor-changing axial current by choosing the upper 3×3 block of $\bar{\lambda}$ to be the Gell-Mann matrices. This choice merely corresponds to an axial transition operator that only acts in the valence sector and is precisely what is implemented on the lattice.[2]

Having fixed the $\bar{\lambda}$ supermatrices, we map the PQQCD axial-current operator into the heavy baryon PQχPT. At leading order, the PQχPT axial current is given by [10]

$$\begin{aligned} J^a_{\mu,5} = {} & 2\alpha(\bar{\mathcal{B}}S_\mu\mathcal{B}\bar{\lambda}^a_{\xi+}) + 2\beta(\bar{\mathcal{B}}S_\mu\bar{\lambda}^a_{\xi+}\mathcal{B}) \\ & + 2\mathcal{H}(\bar{\mathcal{T}}^\nu S_\mu\bar{\lambda}^a_{\xi+}\mathcal{T}_\nu) + \sqrt{\frac{3}{2}}\mathcal{C}[(\bar{\mathcal{T}}_\mu\bar{\lambda}^a_{\xi+}\mathcal{B}) \\ & + (\bar{\mathcal{B}}\bar{\lambda}^a_{\xi+}\mathcal{T}_\mu)], \end{aligned} \tag{24}$$

with α, β, $\mathcal{H}$, and $\mathcal{C}$ the same low-energy constants appearing in Eq. (22) and $\bar{\lambda}^a_{\xi+} = \frac{1}{2}(\xi\bar{\lambda}^a\xi^\dagger + \xi^\dagger\bar{\lambda}^a\xi)$. Since we work to next-to-leading order (NLO) in the chiral expansion and NLO in the momentum expansion, we further require the contributions to the matrix elements from NLO axial current. At NLO, there are two contributions to the axial matrix elements: one is from the NLO axial current in the baryon sector and the other is obtained from the local counterterms involving one insertion of the

[2] Isospin symmetry allows one to relate isospin transition matrix elements to differences of flavor conserving matrix elements. These difference have often been calculated on the lattice. For strangeness transitions, $SU(3)$ is badly broken disallowing the analogous procedure.

quark mass matrix m_Q. The former is given by

$$J^a_{\mu,5} = \frac{1}{\Lambda_\chi^2}\{2n_\alpha[\partial_\mu\partial_\nu(\bar{\mathcal{B}}S^\nu\mathcal{B}\bar{\lambda}^a_{\xi^+}) - \partial^2(\bar{\mathcal{B}}S_\mu\mathcal{B}\bar{\lambda}^a_{\xi^+})] + 2n_\beta[\partial_\mu\partial_\nu(\bar{\mathcal{B}}S^\nu\bar{\lambda}^a_{\xi^+}\mathcal{B}) - \partial^2(\bar{\mathcal{B}}S_\mu\bar{\lambda}^a_{\xi^+}\mathcal{B})]\}, \tag{25}$$

while the latter reads [10]

$$\begin{aligned} J^{a,m_Q}_{\mu,5} = 16\frac{\lambda}{f^2}[&b_1\bar{\mathcal{B}}^{kji}\{\bar{\lambda}^a_{\xi+}, \mathcal{M}_+\}^n_i S_\mu\mathcal{B}_{njk} + b_2(-)^{(\eta_i+\eta_j)(\eta_k+\eta_n)}\bar{\mathcal{B}}^{kji}\{\bar{\lambda}^a_{\xi+}, \mathcal{M}_+\}^n_k S_\mu\mathcal{B}_{ijn} \\ &+ b_3(-)^{\eta_l(\eta_j+\eta_n)}\bar{\mathcal{B}}^{kji}(\bar{\lambda}^a_{\xi+})^l_i(\mathcal{M}_+)^n_j S_\mu\mathcal{B}_{lnk} + b_4(-)^{\eta_l\eta_j+1}\bar{\mathcal{B}}^{kji}((\bar{\lambda}^a_{\xi+})^l_i(\mathcal{M}_+)^n_j \\ &+ (\mathcal{M}_+)^l_i(\bar{\lambda}^a)^n_j)S_\mu\mathcal{B}_{nlk} + b_5(-)^{\eta_i(\eta_l+\eta_j)}\bar{\mathcal{B}}^{kji}(\bar{\lambda}^a_{\xi+})^l_j(\mathcal{M}_+)^n_i S_\mu\mathcal{B}_{nlk} + b_6\bar{\mathcal{B}}^{kji}(\bar{\lambda}^a_{\xi+})^l_i S_\mu\mathcal{B}_{ljk}\mathrm{str}(\mathcal{M}_+) \\ &+ b_7(-)^{(\eta_i+\eta_j)(\eta_k+\eta_n)}\bar{\mathcal{B}}^{kji}(\bar{\lambda}^a_{\xi+})^n_k S_\mu\mathcal{B}_{ijn}\mathrm{str}(\mathcal{M}_+) + b_8\bar{\mathcal{B}}^{kji}S_\mu\mathcal{B}_{ijk}\mathrm{str}(\bar{\lambda}^a_{\xi+}\mathcal{M}_+)], \end{aligned} \tag{26}$$

where the coefficients $b_1, b_2\ldots, b_8$ must be determined from lattice simulations. The relation between the partially quenched parameters n_α, n_β and the physical parameters n_D, n_F in usual $SU(3)$ χPT can be obtained by matching: $n_\alpha = \frac{2}{3}n_D + 2n_F$, $n_\beta = -\frac{5}{3}n_D + n_F$. Notice that the operator $b_8\bar{\mathcal{B}}^{kji}S_\mu\mathcal{B}_{ijk}\mathrm{str}(\bar{\lambda}^a_{\xi+}\mathcal{M}_+)$ does not contribute to the flavor-changing transitions at tree level. This leaves seven independent partially quenched NLO operators, one more than that in ordinary $SU(3)$. However, because these counterterms only contribute to tree level, no unphysical combinations will be introduced.

B. Isospin changing transitions

In the partially quenched theory, the supermatrix for the $\Delta I = 1$ isospin changing transitions is

$$\bar{\lambda}^{\,1+2i}_{ij} = \begin{cases} 1 & i=1, j=2 \\ 0 & \text{otherwise.}\end{cases} \tag{27}$$

Within the baryon octet there are six isospin $\Delta I = 1$ changing transitions, namely,

$$\begin{aligned} &n\to p, \qquad \Sigma^0\to\Sigma^+, \qquad \Sigma^-\to\Sigma^0, \\ &\Lambda\to\Sigma^+, \qquad \Sigma^-\to\Lambda, \qquad \Xi^-\to\Xi^0. \end{aligned} \tag{28}$$

The neutron to proton axial transition defines the nucleon axial form factor $G_{A,NN}(q^2)$ and induced pseudoscalar form factor $G_{P,NN}(q^2)$

$$\langle p(P')|J^{1+2i}_{\mu,5}|n(P)\rangle = \bar{U}_N(P')\left[2S_\mu G_{A,NN}(q^2) + \frac{q_\mu q\cdot S}{(2m_N)^2}G_{P,NN}(q^2)\right]U_N(P), \tag{29}$$

where $q_\mu = (P'-P)_\mu$ is the four momentum transfer. The $\Sigma\Sigma$ transition matrix elements define the $\Sigma\Sigma$ axial form factor $G_{A,\Sigma\Sigma}(q^2)$ and induced pseudoscalar form factor $G_{P,\Sigma\Sigma}(q^2)$

$$\langle\Sigma^0(P')|J^{1+2i}_{\mu,5}|\Sigma^-(P)\rangle = \frac{1}{\sqrt{2}}\bar{U}_\Sigma(P')\left[2S_\mu G_{A,\Sigma\Sigma}(q^2) + \frac{q_\mu q\cdot S}{(2m_\Sigma)^2}G_{P,\Sigma\Sigma}(q^2)\right]U_\Sigma(P). \tag{30}$$

While there are two $\Sigma\Sigma$ isospin transitions, their matrix elements are related by isospin algebra

$$\langle\Sigma^+(P')|J^{1+2i}_{\mu,5}|\Sigma^0(P)\rangle = -\langle\Sigma^0(P')|J^{1+2i}_{\mu,5}|\Sigma^-(P)\rangle. \tag{31}$$

The $\Lambda\Sigma$ transition matrix elements define the $\Lambda\Sigma$ axial form factor $G_{A,\Lambda\Sigma}$ and induced pseudoscalar form factor $G_{P,\Lambda\Sigma}(q^2)$

$$\langle\Lambda(P')|J^{1+2i}_{\mu,5}|\Sigma^-(P)\rangle = \frac{1}{\sqrt{6}}\bar{U}_\Lambda(P')\left[2S_\mu G_{A,\Lambda\Sigma}(q^2) + \frac{q_\mu q\cdot S}{(m_\Lambda+m_\Sigma)^2}G_{P,\Lambda\Sigma}(q^2)\right]U_\Sigma(P). \tag{32}$$

Although there are two $\Lambda\Sigma$ transition matrix elements, they are related by isospin

$$\langle\Sigma^+(P')|J^{1+2i}_{\mu,5}|\Lambda(P)\rangle = \langle\Lambda(P')|J^{1+2i}_{\mu,5}|\Sigma^-(P)\rangle. \tag{33}$$

Finally, the $\Xi\Xi$ axial form factor $G_{A,\Xi\Xi}$ and induced pseudoscalar form factor $G_{P,\Lambda\Sigma}(q^2)$ appear in the $\Xi\Xi$ transition matrix element

$$\langle\Xi^0(P')|J^{1+2i}_{\mu,5}|\Xi^-(P)\rangle = \bar{U}_\Xi(P')\left[2S_\mu G_{A,\Xi\Xi}(q^2) + \frac{q_\mu q\cdot S}{(2m_\Xi)^2}G_{P,\Xi\Xi}(q^2)\right]U_\Xi(P). \tag{34}$$

Here we use heavy baryon spinors and notation. One can easily show up to recoil corrections, $2\bar{U}(P')S_\mu U(P) = \bar{U}(P')\gamma_\mu\gamma_5 U(P)$, where on the right-hand side appears ordinary Dirac matrices and spinors. Thus the axial charges, $G_{A,B'B}(0)$, are the standard ones. In our power counting, while the tree-level contributions from the LO axial current is of order ε^0, the tree-level contributions

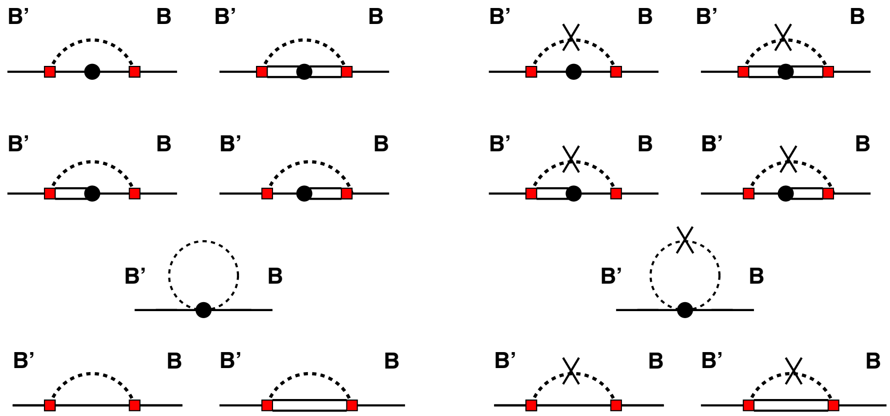

FIG. 1 (color online). One-loop diagrams which contribute to the leading nonanalytic terms of the octet baryon axial form factors. Mesons are represented by a dashed line while the single and double lines are the symbols for an octet and a decuplet, respectively. The solid circle is an insertion of the axial-current operator and the solid squares are the couplings given in Eq. (22). The wave function renormalization diagrams are depicted in the bottom row. The diagrams with a cross on the loop meson are the hairpin contributions which arise from the flavor neutral meson propagators.

obtained from the NLO current count ε^2. In addition, at order ε^2 there are leading nonanalytic contributions to the matrix elements from the one-loop diagrams shown in Figs. 1 and 2. The one-loop diagrams in Fig. 1 contribute to the axial form factors while the induced pseudoscalar form factors receive contributions from the one-loop diagrams in Fig. 2. Evaluation of the diagrams in Fig. 1 together with the tree-level contributions yields the following expression for the axial form factor of $\Delta I = 1$ isospin transition

$$G_{A,B'B}(q^2) = g_{B'B}\sqrt{Z_{B'}Z_B} + \frac{1}{16\pi^2 f^2}\Big[g_{B'B}\sum_\phi C_\phi \mathcal{L}(m_\phi,\mu) + \mathcal{H}\mathcal{C}^2\Big(\sum_\phi E_\phi \mathcal{J}(m_\phi,\Delta,\mu) + \sum_{\phi\phi'}\bar{E}_{\phi\phi'}\mathcal{T}(\eta_\phi\eta_{\phi'},\Delta,\mu)\Big) + \mathcal{C}^2\Big(\sum_\phi A_\phi \mathcal{K}(m_\phi,\Delta,\mu) + \sum_{\phi\phi'}\bar{A}_{\phi\phi'}\mathcal{S}(\eta_\phi\eta_{\phi'},\Delta,\mu)\Big) + \sum_\phi Y_\phi \mathcal{L}(m_\phi,\mu) + \sum_{\phi\phi'}\bar{Y}_{\phi,\phi'}\mathcal{R}(\eta_\phi\eta_{\phi'},\Delta,\mu)\Big] + n_{B'B}\frac{q^2}{\Lambda_\chi^2} + \sum_\phi u_\phi m_\phi^2. \tag{35}$$

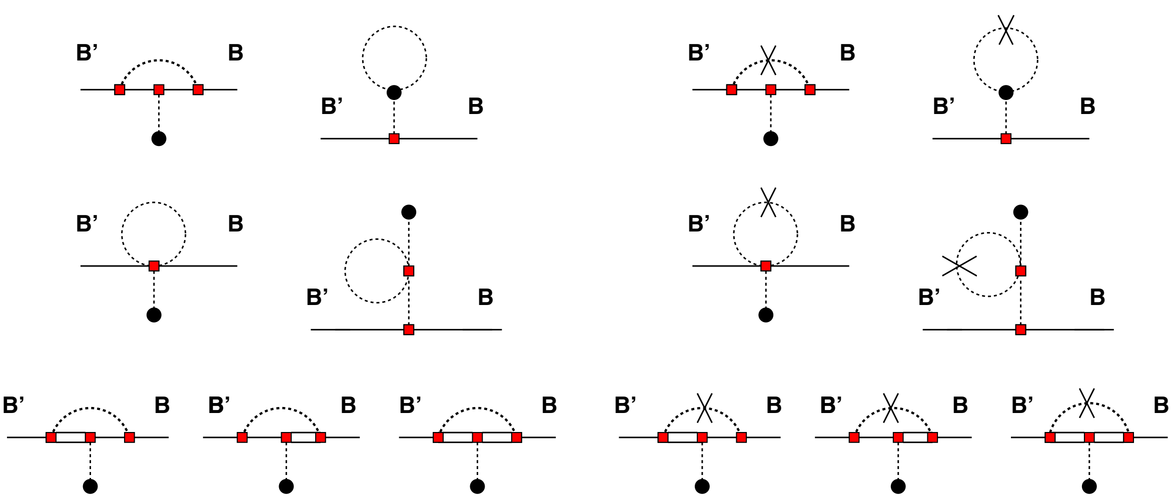

FIG. 2 (color online). One-loop diagrams which contribute to the leading nonanalytic terms of the octet baryon induced pseudoscalar form factors. Diagram elements are the same as Fig. 1.

TABLE I. The coefficients C_ϕ in PQχPT for the isospin changing axial form factors. The C_ϕ are categorized by the loop mesons ϕ with mass m_ϕ and are the same for all isospin transitions.

C_ϕ	
uj	ur
-2	-1

In Eq. (35), B (B') stands for the initial (final) octet baryon, and Z_B and $Z_{B'}$ are the wave function renormalization factors and are given in the appendix. The constants $g_{B'B}$'s are the leading order octet baryon axial charges

$$g_{NN} = (D+F), \qquad g_{\Lambda\Sigma} = 2D, \qquad g_{\Xi\Xi} = (D-F), \qquad g_{\Sigma\Sigma} = 2F, \tag{36}$$

and the coefficients $n_{B'B}$ are given by

$$n_{NN} = n_D + n_F, \qquad n_{\Lambda\Sigma} = 2n_D, \qquad n_{\Xi\Xi} = n_D - n_F, \qquad n_{\Sigma\Sigma} = 2n_F. \tag{37}$$

The coefficients C_ϕ, E_ϕ, $\bar{E}_{\phi\phi'}$, A_ϕ, $\bar{A}_{\phi\phi'}$, Y_ϕ, $\bar{Y}_{\phi\phi'}$, and u_ϕ are given in Tables I, II, III, IV, and V, while the non-analytic functions appearing in Eq. (35), namely, $\mathcal{L}$'s, $\mathcal{J}$'s, $\mathcal{K}$'s, $\mathcal{R}$'s, $\mathcal{T}$'s, and $\mathcal{S}$'s are given by

$$\mathcal{L}(m,\mu) = m^2 \log\left(\frac{m^2}{\mu^2}\right), \tag{38}$$

$$\begin{aligned}\mathcal{K}(m,\Delta,\mu) = {} & \left(m^2 - \frac{2}{3}\Delta^2\right)\log\left(\frac{m^2}{\mu^2}\right) + \frac{2}{3}\Delta\sqrt{\Delta^2-m^2}\log\left(\frac{\Delta-\sqrt{\Delta^2-m^2+i\epsilon}}{\Delta+\sqrt{\Delta^2-m^2+i\epsilon}}\right) \\ & + \frac{2}{3}\frac{m^2}{\Delta}\left(\pi m - \sqrt{\Delta^2-m^2} \times \log\left(\frac{\Delta-\sqrt{\Delta^2-m^2+i\epsilon}}{\Delta+\sqrt{\Delta^2-m^2+i\epsilon}}\right)\right),\end{aligned} \tag{39}$$

$$\mathcal{J}(m,\Delta,\mu) = (m^2 - 2\Delta^2)\log\left(\frac{m^2}{\mu^2}\right) + 2\Delta\sqrt{\Delta^2-m^2}\log\left(\frac{\Delta-\sqrt{\Delta^2-m^2+i\epsilon}}{\Delta+\sqrt{\Delta^2-m^2+i\epsilon}}\right), \tag{40}$$

$$\begin{aligned}\mathcal{R}(\eta_\phi\eta_{\phi'},\Delta,\mu) &= \mathcal{H}(\mathcal{L}(m_{\eta_\phi},\mu), \mathcal{L}(m_{\eta_{\phi'}},\mu), \mathcal{L}(m_X,\mu)), \\ \mathcal{T}(\eta_\phi\eta_{\phi'},\Delta,\mu) &= \mathcal{H}(\mathcal{J}(m_{\eta_\phi},\Delta,\mu), \mathcal{J}(m_{\eta_{\phi'}},\Delta,\mu), \mathcal{J}(m_X,\Delta,\mu)), \\ \mathcal{S}(\eta_\phi\eta_{\phi'},\Delta,\mu) &= \mathcal{H}(\mathcal{K}(m_{\eta_\phi},\Delta,\mu), \mathcal{K}(m_{\eta_{\phi'}}\Delta,\mu), \mathcal{K}(m_X,\Delta,\mu)).\end{aligned} \tag{41}$$

TABLE II. The coefficients E_ϕ and $\bar{E}_{\phi\phi'}$ in PQχPT for the isospin changing axial form factors. The E_ϕ are categorized by the loop mesons ϕ with mass m_ϕ, and $\bar{E}_{\phi\phi'}$ are listed by pairs $\phi\phi'$ of η_q mesons.

E_ϕ								$\bar{E}_{\phi\phi'}$		
	η_u	η_s	us	uj	ur	sj	sr	$\eta_u\eta_u$	$\eta_u\eta_s$	$\eta_s\eta_s$
NN	$-\frac{20}{27}$	0	0	$-\frac{40}{81}$	$-\frac{20}{81}$	0	0	0	0	0
$\Lambda\Sigma$	$-\frac{10}{27}$	0	$-\frac{10}{54}$	$-\frac{10}{27}$	$-\frac{10}{54}$	0	0	0	0	0
$\Xi\Xi$	0	$\frac{5}{81}$	$\frac{10}{81}$	0	0	$\frac{10}{81}$	$\frac{5}{81}$	$\frac{10}{81}$	$-\frac{20}{81}$	$\frac{10}{81}$
$\Sigma\Sigma$	$-\frac{10}{81}$	0	$-\frac{65}{81}$	$-\frac{10}{81}$	$-\frac{5}{81}$	$-\frac{40}{81}$	$-\frac{20}{81}$	$-\frac{20}{81}$	$\frac{40}{81}$	$-\frac{20}{81}$

TABLE III. The coefficients A_ϕ and $\bar{A}_{\phi\phi'}$ in PQχPT for the isospin changing axial form factors. The A_ϕ and $\bar{A}_{\phi\phi'}$ coefficients are categorized as in Table II.

A_ϕ					$\bar{A}_{\phi\phi'}$	
	η_u	η_s	us	uj	$\eta_u\eta_u$	$\eta_u\eta_s$
NN	$\frac{8}{9}D+\frac{8}{3}F$	0	0	$\frac{8}{3}D+\frac{8}{9}F$	0	0
$\Lambda\Sigma$	$-\frac{4}{9}D+\frac{4}{3}F$	0	$\frac{16}{9}D+\frac{8}{3}F$	$\frac{16}{9}D$	$\frac{16}{9}D-\frac{8}{3}F$	$-\frac{20}{9}D+\frac{4}{3}F$
$\Xi\Xi$	0	$\frac{8}{9}F$	$\frac{4}{9}D+\frac{4}{9}F$	0	$\frac{8}{9}D-\frac{8}{9}F$	$-\frac{8}{9}D-\frac{8}{9}F$
$\Sigma\Sigma$	$\frac{8}{9}F$	0	$\frac{4}{9}D+\frac{4}{9}F$	$\frac{8}{9}D+\frac{8}{9}F$	$\frac{16}{9}F$	$-\frac{8}{9}D-\frac{8}{9}F$
	ur	sj	sr		$\eta_s\eta_s$	
NN	$\frac{4}{3}D+\frac{4}{9}F$	0	0		0	
$\Lambda\Sigma$	$\frac{8}{9}D$	$\frac{8}{9}D+\frac{8}{3}F$	$\frac{4}{9}D+\frac{4}{3}F$		$\frac{4}{9}D+\frac{4}{3}F$	
$\Xi\Xi$	0	$\frac{16}{9}F$	$\frac{8}{9}F$		$\frac{16}{9}F$	
$\Sigma\Sigma$	$\frac{4}{9}D+\frac{4}{9}F$	$\frac{16}{9}D-\frac{16}{9}F$	$\frac{8}{9}D-\frac{8}{9}F$		$\frac{8}{9}D-\frac{8}{9}F$	

TABLE IV. The coefficients Y_ϕ and $\bar{Y}_{\phi\phi'}$ in PQχPT for the isospin changing axial form factors. The Y_ϕ and $\bar{Y}_{\phi\phi'}$ coefficients are categorized as in Table II.

Y_ϕ			$\bar{Y}_{\phi\phi'}$
	η_u	η_s	$\eta_u\eta_u$
NN	$-\frac{4}{3}D^3+\frac{16}{3}D^2F-4DF^2$	0	$-D^3+5D^2F-3DF^2-9F^3$
$\Lambda\Sigma$	$-\frac{16}{9}D^3+\frac{16}{3}D^2F$	0	$\frac{16}{3}D^2F-8DF^2$
$\Xi\Xi$	0	$-\frac{2}{9}D^3-\frac{2}{3}D^2F-2DF^2+2F^3$	$-D^3+3D^2F-3DF^2+F^3$
$\Sigma\Sigma$	$-\frac{8}{9}D^3+\frac{4}{3}D^2F-4F^3$	0	$-8F^3$
	us	uj	$\eta_u\eta_s$
NN	0	$\frac{4}{3}D^3-\frac{4}{3}D^2F+4DF^2-4F^3$	0
$\Lambda\Sigma$	$\frac{4}{9}D^3-\frac{4}{3}D^2F$	$\frac{4}{9}D^3-\frac{8}{3}D^2F+4DF^2$	$-\frac{8}{3}D^3+\frac{16}{3}D^2F-8DF^2$
$\Xi\Xi$	$\frac{2}{9}D^3-\frac{2}{3}D^2F+6DF^2-2F^3$	0	$4D^2F-8DF^2+4F^3$
$\Sigma\Sigma$	$-\frac{4}{9}D^3+\frac{16}{3}D^2F-8DF^2+4F^3$	$\frac{8}{9}D^3+\frac{4}{3}D^2F-4F^3$	$8DF^2-8F^3$
	ur	sj	$\eta_s\eta_s$
NN	$\frac{2}{3}D^3-\frac{2}{3}D^2F+2DF^2-2F^3$	0	0
$\Lambda\Sigma$	$\frac{2}{9}D^3-\frac{4}{3}D^2F+2DF^2$	$\frac{4}{3}D^3+\frac{8}{3}D^2F-4DF^2$	$\frac{2}{3}D^3+\frac{4}{3}D^2F-2DF^2$
$\Xi\Xi$	0	$\frac{4}{9}D^3+\frac{4}{3}D^2F-4DF^2+4F^3$	$-4DF^2+4F^3$
$\Sigma\Sigma$	$\frac{4}{9}D^3+\frac{2}{3}D^2F-2F^3$	$-4D^2F+8DF^2-4F^3$	$-2D^2F+4DF^2-2F^3$
	sr		
NN	0		
$\Lambda\Sigma$	$\frac{2}{3}D^3+\frac{4}{3}D^2F-2DF^2$		
$\Xi\Xi$	$\frac{2}{9}D^3+\frac{2}{3}D^2F-2DF^2+2F^3$		
$\Sigma\Sigma$	$-2D^2F+4DF^2-2F^3$		

At NLO, the momentum behavior of the axial form factors is purely polynomial. This in turn implies that the axial radii $\langle r^2_{B'B}\rangle$, which are defined by $\langle r^2_{B'B}\rangle \equiv \lim_{q\to 0} 6\frac{d}{dq^2}G_{A,B'B}(q^2)$, are insensitive to NLO chiral corrections. Since no q^2 dependence appears in the nonanalytic functions from one-loop diagrams, the axial form factors are insensitive to the long-range effects introduced by boundary conditions. Therefore, flavor twisted boundary conditions can be used to produce momentum transfer between initial and final baryon states without sizable finite volume corrections to the extraction of the axial radii [48].

The one-loop diagrams which contribute at NLO to the pseudoscalar form factor are depicted in Fig. 2. Additionally there are further diagrams generated by the insertion of local interactions from the fourth-order meson Lagrangian. Despite the large number of diagrams, there are a number of simplifications. In particular the second and fourth diagrams of the second line in Fig. 2 (along with local insertions on the meson line) lead to the one-loop renormalized pion propagator. Additionally the second and fourth diagrams of the first row in Fig. 2 (along with NLO pion axial coupling) contribute to the one-loop value of the pion decay constant. The remaining ten diagrams are generated from vertices in the NLO baryon Lagrangian. These diagrams renormalize the tree-level axial coupling of the pion to the baryons. Carefully accounting for all of these factors, we find

$$G_{P,B'B}(q^2) = (m_B + m_{B'})^2\bigg(\frac{f_\pi/f}{q^2 - m_\pi^2}G_{A,B'B}(0)\sqrt{Z_\pi} - \frac{1}{3}\langle r^2_{B'B}\rangle\bigg), \tag{42}$$

where in this NLO expression, the axial charge $G_{A,B'B}(0)$, pion mass m_π, and pion decay constant f_π are taken to be their physical values and Z_π is the pion wave function renormalization which is shown in the appendix. In fitting lattice data to Eq. (42), one would thus use the lattice

TABLE V. The coefficients u_ϕ in PQχPT for the isospin changing axial form factors. The u_ϕ coefficients are categorized by the mesons with mass m_ϕ.

u_ϕ				
	uu	ss	jj	rr
NN	$-\frac{1}{3}b_1+\frac{2}{3}b_2-\frac{1}{6}b_3+\frac{1}{6}b_4+\frac{1}{3}b_5$	0	$\frac{2}{3}b_7-\frac{1}{3}b_6$	$\frac{1}{3}b_7-\frac{1}{6}b_6$
$\Lambda\Sigma$	$-b_1+\frac{1}{2}b_2-\frac{1}{4}b_3+\frac{1}{4}b_5$	$-\frac{1}{4}b_3+\frac{1}{2}b_4$	$\frac{1}{2}b_7-b_6$	$\frac{1}{4}b_7-\frac{1}{2}b_6$
$\Xi\Xi$	$-\frac{2}{3}b_1-\frac{1}{6}b_2$	$-\frac{1}{3}b_3+\frac{1}{3}b_4-\frac{1}{12}b_5$	$-\frac{1}{6}b_7-\frac{2}{3}b_6$	$-\frac{1}{12}b_7-\frac{1}{3}b_6$
$\Sigma\Sigma$	$\frac{1}{3}b_1+\frac{5}{6}b_2+\frac{1}{12}b_3+\frac{1}{6}b_4+\frac{1}{12}b_5$	$\frac{1}{12}b_3-\frac{1}{3}b_4+\frac{1}{3}b_5$	$\frac{5}{6}b_7+\frac{1}{3}b_6$	$\frac{5}{12}b_7+\frac{1}{6}b_6$

measured values for $G_{A,B'B}(0)$, m_π, and f_π. The final term in the pseudoscalar form factor is $\langle r^2_{B'B}\rangle$, which is the axial radius. Its appearance here was discovered long ago under the guise of partially conserved axial-vector current hypothesis (PCAC) by Adler and Dothan [49].

The simple structure of the psuedoscalar form factor at NLO in both χPT and PQχPT allows one to perform an approximate check of the Goldberger-Treiman relation. The residue of the pseudoscalar form factor at the pion pole is proportional to the pion-baryon-baryon coupling $G_{\pi B'B}$. One can thus perturbatively investigate the Goldberger-Treiman relation using a lattice determination of the pseudoscalar form factor. This indirect method is considerably simpler than a lattice measurement of baryon-to-baryon-plus-pion correlation functions which contain final state interactions.

C. Strangeness changing transitions

The $\Delta S = -1$ strangeness changing transitions corresponds to the flavor matrix $\bar\lambda^{4+5i}$ which is given by

$$\bar\lambda^{4+5i}_{ij} = \begin{cases} 1 & i=1, j=3 \\ 0 & \text{otherwise,} \end{cases} \tag{43}$$

in the partially quenched theory. With Eq. (43) there exist six strangeness changing transitions among the hyperons

$$\begin{aligned} &\Sigma^0 \to p, \qquad \Sigma^- \to n, \qquad \Lambda \to p, \\ &\Xi^0 \to \Sigma^+, \qquad \Xi^- \to \Sigma^0, \qquad \Xi^- \to \Lambda. \end{aligned} \tag{44}$$

The $N\Lambda$ transition matrix elements define the $N\Lambda$ axial form factor $G_{A,N\Lambda}(q^2)$ and induced pseudoscalar form factor $G_{P,N\Lambda}(q^2)$

$$\langle p(P')|J^{4+5i}_{\mu,5}|\Lambda(P)\rangle = -\frac{1}{\sqrt{6}}\bar U_N(P')\bigg[2S_\mu G_{A,N\Lambda}(q^2) + \frac{q_\mu q\cdot S}{(m_N+m_\Lambda)^2}G_{P,N\Lambda}(q^2)\bigg]U_\Lambda(P), \tag{45}$$

where, as above, $q_\mu = (P'-P)_\mu$ is the four momentum transfer. The $\Lambda\Xi$ transition matrix elements define the $\Lambda\Xi$ axial form factor $G_{A,\Lambda\Xi}(q^2)$ and induced pseudoscalar form factor $G_{P,\Lambda\Xi}(q^2)$

$$\langle \Lambda(P')|J^{4+5i}_{\mu,5}|\Xi^-(P)\rangle = \frac{1}{\sqrt{6}}\bar U_\Lambda(P')\bigg[2S_\mu G_{A,\Lambda\Xi}(q^2) + \frac{q_\mu q\cdot S}{(m_\Lambda+m_\Xi)^2}G_{P,\Lambda\Xi}(q^2)\bigg]U_\Xi(P). \tag{46}$$

The $N\Sigma$ axial transitions defines the $N\Sigma$ axial form factor $G_{A,N\Sigma}(q^2)$ and the induced pseudoscalar form factor $G_{P,N\Sigma}(q^2)$

$$\langle n(P')|J^{+}_{\mu,5}|\Sigma^-(P)\rangle = \bar U_N(P')\bigg[2S_\mu G_{A,N\Sigma}(q^2) + \frac{q_\mu q\cdot S}{(m_N+m_\Sigma)^2}G_{P,N\Sigma}(q^2)\bigg]U_\Sigma(P). \tag{47}$$

Finally, the $\Sigma\Xi$ axial form factor $G_{A,\Sigma\Xi}(q^2)$ and the induced pseudoscalar form factor $G_{P,\Sigma\Xi}(q^2)$ is defined through the $\Sigma\Xi$ transition matrix element

$$\langle \Sigma^0(P')|J^{4+5}_{\mu,5}|\Xi^-(P)\rangle = \frac{1}{\sqrt{2}}\bar U_\Sigma(P')\bigg[2S_\mu G_{A,\Sigma\Xi}(q^2) + \frac{q_\mu q\cdot S}{(m_\Sigma+m_\Xi)^2}G_{P,\Sigma\xi}(q^2)\bigg]U_\Xi(P). \tag{48}$$

Notice while there are two $N\Sigma$ and two $\Sigma\Xi$ transitions, both of their matrix elements are related by isospin factors, namely,

$$\begin{aligned} \langle p(P')|J^{4+5i}_{\mu,5}|\Sigma^0(P)\rangle &= \frac{1}{\sqrt{2}}\langle n(P')|J^{4+5i}_{\mu,5}|\Sigma^-(P)\rangle, \\ \langle \Sigma^0(P')|J^{4+5i}_{\mu,5}|\Xi^-(P)\rangle &= \frac{1}{\sqrt{2}}\langle \Sigma^+(P')|J^{4+5i}_{\mu,5}|\Xi^0(P)\rangle. \end{aligned} \tag{49}$$

Following the same considerations in Sec. III B and assembling the LO and NLO contributions, the axial form factors of strangeness changing transitions are given by

$$\begin{aligned} G_{A,B'B}(q^2) = {}& g_{B'B}\sqrt{Z_{B'}Z_B} + \frac{1}{16\pi^2 f^2}\bigg[g_{B'B}\bigg(\sum_\phi C_\phi \mathcal{L}(m_\phi,\mu) + \sum_{\phi\phi'}\bar C_{\phi\phi'}\mathcal{R}(\eta_\phi\eta_{\phi'},\Delta,\mu)\bigg) + \mathcal{H}\mathcal{C}^2\bigg(\sum_\phi E_\phi \mathcal{J}(m_\phi,\Delta,\mu) \\ & + \sum_{\phi\phi'}\bar E_{\phi\phi'}\mathcal{T}(\eta_\phi\eta_{\phi'},\Delta,\mu)\bigg) + \mathcal{C}^2\bigg(\sum_\phi A_\phi\mathcal{K}(m_\phi,\Delta,\mu) + \sum_{\phi\phi'}\bar A_{\phi\phi'}\mathcal{S}(\eta_\phi\eta_{\phi'},\Delta,\mu)\bigg) \\ & + \sum_\phi Y_\phi\mathcal{L}(m_\phi,\mu) + \sum_{\phi\phi'}\bar Y_{\phi,\phi'}\mathcal{R}(\eta_\phi\eta_{\phi'},\Delta,\mu)\bigg] + n_{B'B}\frac{q^2}{\Lambda_\chi^2} + \sum_\phi u_\phi m_\phi^2. \end{aligned} \tag{50}$$

In Eq. (50), we use B and B' to denote the initial and final states of octet baryon, and Z_B and $Z_{B'}$ are again the wave function renormalization for which the explicit expressions are given in the appendix. The $g_{B'B}$'s appearing above are the leading order octet baryon axial charges

TABLE VI. The coefficients C_ϕ and $\bar{C}_{\phi\phi'}$ in PQχPT, which are all the same for the strangeness changing axial form factors. The C_ϕ and $\bar{C}_{\phi\phi'}$ coefficients are categorized as in Table II.

C_ϕ				$\bar{C}_{\phi\phi'}$		
uj	ur	sj	sr	$\eta_u\eta_u$	$\eta_u\eta_s$	$\eta_s\eta_s$
-1	$-\frac{1}{2}$	-1	$-\frac{1}{2}$	$-\frac{1}{2}$	1	$-\frac{1}{2}$

$$
\begin{aligned}
g_{N\Lambda} &= (3F + D), \qquad g_{\Lambda\Xi} = (3F - D), \\
g_{N\Sigma} &= (D - F), \qquad g_{\Sigma\Xi} = (F + D),
\end{aligned} \tag{51}
$$

and the coefficients $n_{B'B}$ are given by a formula of exactly the same form

$$
\begin{aligned}
n_{N\Lambda} &= 3n_F + n_D, \qquad n_{\Lambda\Xi} = 3n_F - n_D, \\
n_{N\Sigma} &= n_D - n_F, \qquad n_{\Sigma\Xi} = n_D + n_F.
\end{aligned} \tag{52}
$$

The coefficientsC_ϕ, $\bar{C}_{\phi\phi'}$, E_ϕ, $\bar{E}_{\phi\phi'}$, A_ϕ, $\bar{A}_{\phi\phi'}$, Y_ϕ, $\bar{Y}_{\phi\phi'}$, and u_ϕ are given in Tables VI, VII, VIII, IX, and X. Finally, the nonanalytic functions $\mathcal{L}$'s, $\mathcal{J}$'s, $\mathcal{K}$'s, $\mathcal{R}$'s, $\mathcal{T}$'s, and $\mathcal{S}$'s in the above equations are defined in Sec. III B. Employing the same argument as one did in deriving the isospin changing pseudoscalar form factors, one arrives at a similar expression for the strangeness changing pseudoscalar form factor

$$
G_{P,B'B}(q^2) = (m_B + m_{B'})^2\left(\frac{f_K/f}{q^2 - m_K^2} G_{A,B'B}(0)\sqrt{Z_K} - \frac{1}{3}\langle r^2_{B'B}\rangle\right), \tag{53}
$$

where in this NLO expression, the axial charge $G_{A,B'B}(0)$, kaon mass m_K, and kaon decay constant f_K are taken to be their physical values, and Z_K is the kaon wave function renormalization which is shown in the appendix. In fitting lattice data to Eq. (53), one would thus use the lattice measured values for $G_{A,B'B}(0)$, m_K, and f_K. The final term in the pseudoscalar form factor is $\langle r^2_{B'B}\rangle$, which is the strangeness changing axial radius. As has been shown in Sec. III B, the simple structure of the psuedoscalar form factor at NLO in both χPT and PQχPT allows one to perform an approximate check of the Goldberger-Treiman relation. Here the residue of the pseudoscalar form factor at the kaon pole is proportional to the kaon-baryon-baryon coupling $G_{KB'B}$; thus the pseudoscalar form factor provides an indirect and simple method to investigate the Goldberger-Treiman relation on the lattice.

IV. DISCUSSION

Above we have calculated the full set of flavor-changing axial-current matrix elements of the hyperons. The expressions will be useful for the study of the chiral and momentum behavior of hyperon axial form factors using lattice QCD.

TABLE VII. The coefficients E_ϕ and $\bar{E}_{\phi\phi'}$ in PQχPT for the strangeness changing axial form factors. The E_ϕ and $\bar{E}_{\phi\phi'}$ coefficients are categorized as in Table II.

E_ϕ								$\bar{E}_{\phi\phi'}$		
	η_u	η_s	us	uj	ur	sj	sr	$\eta_u\eta_u$	$\eta_u\eta_s$	$\eta_s\eta_s$
$N\Lambda$	$-\frac{10}{9}$	0	$-\frac{10}{18}$	$-\frac{10}{9}$	$-\frac{10}{18}$	0	0	0	0	0
$\Lambda\Xi$	$-\frac{10}{27}$	0	$-\frac{20}{27}$	$-\frac{20}{27}$	$-\frac{10}{27}$	0	0	0	0	0
$N\Sigma$	$\frac{10}{81}$	0	$\frac{5}{81}$	$\frac{10}{81}$	$\frac{5}{81}$	0	0	0	0	0
$\Sigma\Xi$	$-\frac{10}{81}$	$-\frac{10}{81}$	$-\frac{40}{81}$	$-\frac{20}{81}$	$-\frac{10}{81}$	$-\frac{20}{81}$	$-\frac{10}{81}$	$-\frac{20}{81}$	$\frac{40}{81}$	$-\frac{20}{81}$

TABLE VIII. The coefficients A_ϕ and $\bar{A}_{\phi\phi'}$ in PQχPT for the strangeness changing axial form factors. The A_ϕ and $\bar{A}_{\phi\phi'}$ coefficients are categorized as in Table II.

A_ϕ					$\bar{A}_{\phi\phi'}$	
	η_u	η_s	us	uj	$\eta_u\eta_u$	$\eta_u\eta_s$
$N\Lambda$	$2D + 2F$	0	$-\frac{2}{3}D + 2F$	$\frac{16}{3}D$	0	0
$\Lambda\Xi$	$-\frac{2}{3}D + \frac{2}{3}F$	$\frac{2}{9}D + \frac{2}{3}F$	$\frac{4}{9}D - \frac{4}{3}F$	$\frac{20}{9}D - 4F$	$\frac{16}{9}D - \frac{8}{3}F$	$-\frac{20}{9}D + \frac{4}{3}F$
$N\Sigma$	$\frac{2}{9}D + \frac{10}{9}F$	0	$\frac{2}{9}D + \frac{2}{9}F$	$\frac{16}{9}F$	$-\frac{4}{9}D + \frac{4}{3}F$	$\frac{4}{9}D - \frac{4}{3}F$
$\Sigma\Xi$	$-\frac{2}{9}D + \frac{2}{9}F$	$-\frac{2}{9}D + \frac{2}{9}F$	$\frac{4}{3}D + \frac{20}{9}F$	$\frac{4}{3}D + \frac{4}{9}F$	$\frac{4}{9}D + \frac{4}{9}F$	$-\frac{8}{9}D - \frac{8}{9}F$
	ur	sj	sr		$\eta_s\eta_s$	
$N\Lambda$	$\frac{8}{3}D$	0	0		0	
$\Lambda\Xi$	$\frac{10}{9}D - 2F$	$\frac{4}{9}D + \frac{4}{3}F$	$\frac{2}{9}D + \frac{2}{3}F$		$\frac{4}{9}D + \frac{4}{3}F$	
$N\Sigma$	$\frac{8}{9}F$	0	0		0	
$\Sigma\Xi$	$\frac{2}{3}D + \frac{2}{9}F$	$\frac{4}{3}D + \frac{4}{9}F$	$\frac{2}{3}D + \frac{2}{9}F$		$\frac{4}{9}D + \frac{4}{9}F$	

TABLE IX. The coefficients Y_ϕ and $\bar{Y}_{\phi\phi'}$ in PQχPT for the strangeness changing axial form factors. The Y_ϕ and $\bar{Y}_{\phi\phi'}$ coefficients are categorized as in Table II.

Y_ϕ			$\bar{Y}_{\phi\phi'}$
	η_u	η_s	$\eta_u\eta_u$
$N\Lambda$	$\frac{1}{9}D^3 + 5D^2F - 9DF^2 + 3F^3$	0	$-\frac{4}{3}D^3 + 2D^2F + 12DF^2 - 18F^3$
$\Lambda\Xi$	$-\frac{5}{3}D^3 + \frac{11}{3}D^2F - 5DF^2 + 3F^3$	$-\frac{5}{9}D^3 - D^2F + DF^2 - 3F^3$	$\frac{4}{3}D^3 - \frac{22}{3}D^2F + 12DF^2 - 6F^3$
$N\Sigma$	$-\frac{1}{9}D^3 - D^2F + DF^2 + F^3$	0	$2D^2F - 8DF^2 + 6F^3$
$\Sigma\Xi$	$-\frac{1}{3}D^3 + \frac{7}{3}D^2F - DF^2 - F^3$	$-\frac{1}{3}D^3 + \frac{7}{3}D^2F - DF^2 - F^3$	$2D^2F - 2F^3$
	us	uj	$\eta_u\eta_s$
$N\Lambda$	$-\frac{25}{9}D^3 + 7D^2F - 3DF^2 - 3F^3$	$\frac{20}{9}D^3 - 4D^2F + 12DF^2 - 12F^3$	$\frac{1}{3}D^3 + D^2F - 3DF^2 - 9F^3$
$\Lambda\Xi$	$\frac{8}{9}D^3 + \frac{16}{3}D^2F - 8DF^2$	$-\frac{2}{3}D^3 - \frac{22}{3}D^2F + 14DF^2 - 6F^3$	$-\frac{1}{3}D^3 - \frac{7}{3}D^2F + 15DF^2 - 15F^3$
$N\Sigma$	$\frac{1}{9}D^3 - \frac{1}{3}D^2F + 3DF^2 - F^3$	$\frac{4}{9}D^3 + \frac{4}{3}D^2F - 4DF^2 + 4F^3$	$-D^3 + 5D^2F - 7DF^2 + 3F^3$
$\Sigma\Xi$	$-\frac{2}{3}D^3 + \frac{2}{3}D^2F - 2DF^2 + 2F^3$	$\frac{2}{3}D^3 - \frac{2}{3}D^2F + 2DF^2 - 2F^3$	$-D^3 + D^2F - 3DF^2 - 5F^3$
	ur	sj	$\eta_s\eta_s$
$N\Lambda$	$\frac{10}{9}D^3 - 2D^2F + 6DF^2 - 6F^3$	0	0
$\Lambda\Xi$	$-\frac{1}{3}D^3 - \frac{11}{3}D^2F + 7DF^2 - 3F^3$	$\frac{10}{9}D^3 + \frac{10}{3}D^2F - 2DF^2 - 6F^3$	$\frac{2}{3}D^2F - 6F^3$
$N\Sigma$	$\frac{2}{9}D^3 + \frac{2}{3}D^2F - 2DF^2 + 2F^3$	0	0
$\Sigma\Xi$	$\frac{1}{3}D^3 - \frac{1}{3}D^2F + DF^2 - F^3$	$\frac{2}{3}D^3 - \frac{2}{3}D^2F + 2DF^2 - 2F^3$	$2D^2F - 2F^3$
	sr		
$N\Lambda$	0		
$\Lambda\Xi$	$\frac{5}{9}D^3 + \frac{5}{3}D^2F - DF^2 - 3F^3$		
$N\Sigma$	0		
$\Sigma\Xi$	$\frac{1}{3}D^3 - \frac{1}{3}D^2F + DF^2 - F^3$		

Considering the axial charges of hyperons and of their transitions, there are only two parameters which survive the chiral limit, namely, D and F. As there are eight such charges, there are six relations among them. Focusing just on the isospin and strangeness transitions individually, we have four of the six relations:

$$g_{NN} + g_{\Xi\Xi} - g_{\Lambda\Sigma} = 0, \tag{54}$$

$$g_{NN} - g_{\Xi\Xi} - g_{\Sigma\Sigma} = 0, \tag{55}$$

$$g_{N\Lambda} + g_{\Lambda\Xi} - 3(g_{\Sigma\Xi} - g_{N\Sigma}) = 0, \tag{56}$$

and

$$g_{N\Lambda} - g_{\Lambda\Xi} - g_{N\Sigma} - g_{\Sigma\Xi} = 0. \tag{57}$$

Combining isospin and strangeness transitions together, we arrive at the final two relations:

$$g_{N\Lambda} + g_{\Lambda\Xi} - 3g_{\Sigma\Sigma} = 0, \tag{58}$$

and

$$g_{N\Lambda} - g_{\Lambda\Xi} - g_{\Lambda\Sigma} = 0. \tag{59}$$

These relations hold in $SU(3)$ χPT, as well as $SU(6|3)$ PQχPT. Of course chiral corrections modify these relations and the "0" should be interpreted as $\mathcal{O}(m_\phi^2/\Lambda_\chi^2)$. The expressions derived above in Secs. III B and III C provide these $\mathcal{O}(m_\phi^2/\Lambda_\chi^2)$ corrections which are generally linear combinations of nonanalytic loop contributions and unknown local counterterms.

The relations in Eqs. (54)–(57) actually apply not only to the axial charges, but also to the respective hyperon transition matrix elements as a whole. The pseudoscalar form factors do not satisfy Eqs. (58) and (59) due to the difference in pion versus kaon poles. The axial form factors, by contrast, satisfy these latter two relations.

Apart from the axial couplings D, F, $\mathcal{C}$, $\mathcal{H}$, and meson masses, the axial charges depend on six (eight) unknown parameters in χPT (PQχPT). This lack of predictive power historically has been overlooked by supposing, what has

TABLE X. The coefficients u_ϕ in PQχPT for the strangeness changing axial form factors. The coefficients u_ϕ are categorized by the mesons with mass m_ϕ.

u_ϕ				
	uu	ss	jj	rr
$N\Lambda$	$\frac{3}{4}b_2 + \frac{3}{4}b_5$	$\frac{3}{4}b_2$	$\frac{3}{2}b_7$	$\frac{3}{4}b_7$
$\Lambda\Xi$	$\frac{1}{2}b_1 + \frac{1}{2}b_2 + \frac{1}{4}b_3 - \frac{3}{4}b_4 + \frac{1}{2}b_5$	$\frac{1}{2}b_1 + \frac{1}{2}b_2 + \frac{1}{4}b_3 + \frac{1}{4}b_4$	$b_7 + b_6$	$\frac{1}{2}b_7 + \frac{1}{2}b_6$
$N\Sigma$	$-\frac{1}{3}b_1 - \frac{1}{12}b_2 - \frac{1}{3}b_3 + \frac{1}{3}b_4 - \frac{1}{12}b_5$	$-\frac{1}{3}b_1 - \frac{1}{12}b_2$	$-\frac{1}{6}b_7 - \frac{2}{3}b_6$	$-\frac{1}{12}b_7 - \frac{1}{3}b_6$
$\Sigma\Xi$	$-\frac{1}{6}b_1 + \frac{1}{3}b_2 - \frac{1}{12}b_3 + \frac{1}{12}b_4 + \frac{1}{6}b_5$	$-\frac{1}{6}b_1 + \frac{1}{3}b_2 - \frac{1}{12}b_3 + \frac{1}{12}b_4 + \frac{1}{6}b_5$	$\frac{2}{3}b_7 - \frac{1}{3}b_6$	$\frac{1}{3}b_7 - \frac{1}{6}b_6$

been termed, the formal dominance of chiral logarithms. One can do slightly better and attempt model estimation of these parameters, but the fact stands that most chiral analyses have seriously lacked the ability to make complete predictions. This is the great advantage of lattice QCD calculations, which have the promise to determine the complete information about the low-energy constants.

Despite the absence of knowledge concerning the eight coupling constants in the NLO current Eq. (26), we can make two nontrivial predictions at next-to-leading order by eliminating the local terms. The leading local terms are cancelled in the relations Eqs. (54)–(59). Combinations of these relations can be used to eliminate the next-to-leading order local terms. While there are seven contributing terms, only five of them, $b_1, \ldots, b_5$ contribute to the relations. Thus there must exist at least one combination of Eqs. (54)–(59) that is independent of the b_i. Rather fortuitously there are two such nontrivial combinations of axial charges which are independent of these couplings, *viz.*

$$\Delta g \equiv 2g_{NN} - g_{N\Lambda} - g_{N\Sigma} - g_{\Lambda\Sigma} - g_{\Sigma\Sigma} + 2g_{\Sigma\Xi}, \quad (60)$$

$$\Delta G \equiv 2g_{NN} + 2g_{\Xi\Xi} - 2g_{\Lambda\Sigma} + g_{N\Sigma} + g_{\Lambda\Xi} + g_{\Sigma\Xi} - g_{N\Lambda}. \quad (61)$$

These relations are independent of NLO counterterms in both PQχPT and χPT. The expressions for Δg and ΔG in χPT are[3]

$$(4\pi f)^2\Delta g = \tfrac{2}{3}(D^3 + 5D^2F - 6DF^2 - 6F^3)\mathcal{G}[\mathcal{L}] - \mathcal{C}^2[\tfrac{10}{81}\mathcal{H} + \tfrac{1}{6}(D+F)]\mathcal{G}[\mathcal{J}] - \tfrac{2}{9}\mathcal{C}^2(D-F)\mathcal{G}[\mathcal{K}], \quad (62)$$

$$(4\pi f)^2\Delta G = \tfrac{4}{3}D(D^2 - 6F^2)\mathcal{G}[\mathcal{L}] - \tfrac{1}{3}D\mathcal{C}^2\mathcal{G}[\mathcal{J}] + \tfrac{4}{3}F\mathcal{C}^2\mathcal{G}[\mathcal{K}], \quad (63)$$

where the Gell-Mann Okubo linear combination functional is defined by

$$\mathcal{G}[A] = A_\pi - 4A_K + 3A_\eta, \quad (64)$$

for any function $A_\phi = A(m_\phi, \Delta, \mu)$. The quantities Δg and ΔG allow one to test chiral logarithms directly. Accordingly these relations only superficially have scale dependence, and upon the limit of $SU(3)_V$ symmetry, they vanish. With these symmetry breaking relations, we have separated out the short distance physics and hence isolated long-distance chiral corrections. To obtain values for Δg and ΔG, as well as the curve shown in Fig. 3, we have fixed the strange quark mass at its physical value and used the $SU(6)$ values for the axial couplings: $D = 3/4$, $F = 2/3D$, $\mathcal{C} = -2D$, and $\mathcal{H} = -3D$. In particular, we find $\Delta g = -0.0035$ and $\Delta G = -0.017$ at physical pion mass $m_\pi = 140$ MeV.

Four further nontrivial relations, analogous to Δg and ΔG above, exist when one includes charges arising from the strangeness axial-current $\bar{s}\gamma_\mu\gamma_5 s$. These matrix elements have been determined at zero momentum transfer in PQχPT [33]. Determination of these charges requires the calculation of disconnected operator contractions on the lattice. As such contributions are notoriously difficult to determine, we leave it to future work to deduce the remaining symmetry breaking relations.

[3]Partially quenched expressions can be obtained from Eqs. (62) and (63) under the replacements: $\mathcal{G}[\mathcal{L}] \to \mathcal{G}^{\rm PQ}[\mathcal{L}, \mathcal{R}]$, $\mathcal{G}[\mathcal{K}] \to \mathcal{G}^{\rm PQ}[\mathcal{K}, \mathcal{S}]$, and $\mathcal{G}[\mathcal{J}] \to \mathcal{G}^{\rm PQ}[\mathcal{J}, \mathcal{T}]$. The partially quenched functional is given by

$$\mathcal{G}^{\rm PQ}[A, B] = 2A_\pi - 4A_K + 2A_{\eta_s} + 2B_{\eta_u\eta_u} - 4B_{\eta_u\eta_s} + 2B_{\eta_s\eta_s},$$

for any function $A_\phi = A(m_\phi, \Delta, \mu)$ and hairpin function $B_{\eta_\phi\eta_{\phi'}} = B(\eta_\phi\eta_{\phi'}, \Delta, \mu)$. There is no scale dependence in $\mathcal{G}^{\rm PQ}[A, B]$.

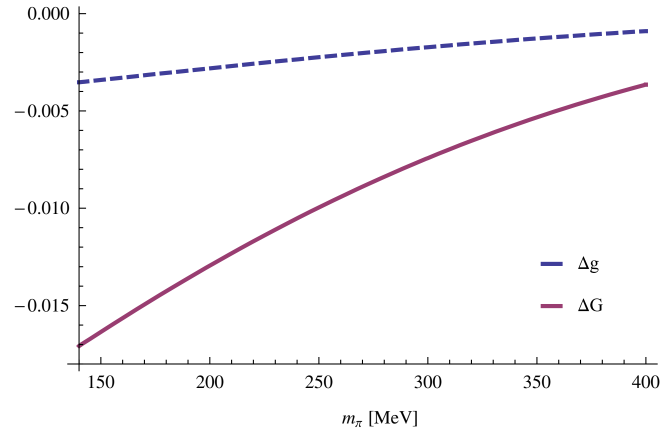

FIG. 3 (color online). Plot of Δg and ΔG as a function of the pion mass m_π.

ACKNOWLEDGMENTS

We thank G. Colangelo for discussions. This work is supported in part by the U.S. Department of Energy, Grants No. DE-FG02-05ER41368-0 and No. DE-FG02-93ER40762 (B. C. T.) and by the Schweizerischer Nationalfonds (F.-J. J.).

APPENDIX: WAVE FUNCTION RENORMALIZATION

In this appendix, we list the necessary wave function renormalization and meson Z-factors appearing in the calculations. For the baryons, we have [39]

$$Z_B = 1 - \frac{1}{16\pi^2 f^2}\left(\sum_\phi \mathcal{A}_\phi \mathcal{L}_\phi + \sum_{\phi,\phi'} \mathcal{A}_{\phi\phi'}\mathcal{R}_{\phi\phi'} + \mathcal{C}^2\left(\sum_\phi \mathcal{B}_\phi \mathcal{J}_\phi + \sum_{\phi,\phi'} \mathcal{B}_{\phi\phi'}\mathcal{T}_{\phi\phi'}\right)\right), \quad (A1)$$

TABLE XI. The coefficients $\mathcal{A}_\phi$ and $\bar{\mathcal{A}}_{\phi\phi'}$ in PQχPT for the wave function renormalization. The $\mathcal{A}_\phi$ and $\bar{\mathcal{A}}_{\phi\phi'}$ coefficients are categorized as in Table II.

$\mathcal{A}_\phi$				$\bar{\mathcal{A}}_{\phi\phi'}$
	η_u	η_s	us	$\eta_u\eta_u$
N	$-4D(D-3F)$	0	0	$3(D-3F)^2$
Λ	$-\frac{2}{3}D^2+8DF-6F^3$	0	$-\frac{10}{3}D^2+4DF+6F^2$	$\frac{4}{3}(2D-3F)^2$
Σ	$2(3F^2-D^2)$	0	$-2(D^2-6DF+3F^2)$	$12F^2$
Ξ	0	$2(3F^2-D^2)$	$-2(D^2-6DF+3F^2)$	$3(D-F)^2$
	uj	ur	js	$\eta_u\eta_s$
N	$10D^2-12DF+18F^2$	$5D^2-6DF+9F^2$	0	0
Λ	$\frac{28}{3}D^2-16DF+12F^2$	$\frac{14}{3}D^2-8DF+6F^2$	$\frac{2}{3}(D+3F)^2$	$-\frac{4}{3}(2D^2+3DF-9F^2)$
Σ	$4D^2+12F^2$	$2D^2+6F^2$	$6(D-F)^2$	$12F(F-D)$
Ξ	$6(D-F)^2$	$3(D-F)^2$	$4(D^2+3F^2)$	$12F(F-D)$
	sr			$\eta_s\eta_s$
N	0			0
Λ	$\frac{1}{3}(D+3F)^2$			$\frac{1}{3}(D+3F)^2$
Σ	$3(D-F)^2$			$3(D-F)^2$
Ξ	$2(D^2+3F^2)$			$12F^2$

TABLE XII. The coefficients $\mathcal{B}_\phi$ and $\bar{\mathcal{B}}_{\phi\phi'}$ in PQχPT for the wave function renormalization. The $\mathcal{B}_\phi$ and $\bar{\mathcal{B}}_{\phi\phi'}$ coefficients are categorized as in Table II.

$\mathcal{B}_\phi$								$\bar{\mathcal{B}}_{\phi\phi'}$		
	η_u	η_s	us	uj	ur	sj	sr	$\eta_u\eta_u$	$\eta_u\eta_s$	$\eta_s\eta_s$
N	2	0	0	2	1	0	0	0	0	0
Λ	1	0	1	2	1	0	0	0	0	0
Σ	$\frac{1}{3}$	0	$\frac{5}{3}$	$\frac{2}{3}$	$\frac{1}{3}$	$\frac{4}{3}$	$\frac{2}{3}$	$\frac{2}{3}$	$-\frac{4}{3}$	$\frac{2}{3}$
Ξ	0	$\frac{1}{3}$	$\frac{5}{3}$	$\frac{4}{3}$	$\frac{2}{3}$	$\frac{2}{3}$	$\frac{1}{3}$	$\frac{2}{3}$	$-\frac{4}{3}$	$\frac{2}{3}$

where the coefficients $\mathcal{A}_\phi$, $\bar{\mathcal{A}}_{\phi,\phi'}$, $\mathcal{B}_\phi$, and $\bar{\mathcal{B}}_{\phi\phi'}$ are given in Tables XI and XII. For the mesons, one has

$$Z_\varphi = 1 + \frac{2}{3}\left(\frac{1}{16\pi^2 f^2}\sum_\phi C_\phi \mathcal{L}(m_\phi,\mu)\right) - \frac{2}{\lambda}((2m_{jj}^2 + m_{rr}^2)\alpha_4 + w_\varphi \alpha_5), \tag{A2}$$

where α_4 and α_5 are the low-energy constants that appear in $\mathcal{L}^4$ in the meson sector. Further, for $\varphi = \pi$, $w_\pi = m_{uu}^2$ and one uses Table I for C_ϕ while for $\varphi = K$, $w_K = m_{us}^2$ and one uses Table VI for C_ϕ. Finally the nonanalytic functions $\mathcal{J}$'s and $\mathcal{L}$'s are given in Sec. III B.

[1] T. DeGrand and C. DeTar, *Lattice Methods for Quantum Chromadynamics* (World Scientific, Singapore, 2006).
[2] C. W. Bernard and M. F. L. Golterman, Phys. Rev. D **46**, 853 (1992).
[3] C. W. Bernard and M. F. L. Golterman, Phys. Rev. D **49**, 486 (1994).
[4] S. R. Sharpe and N. Shoresh, Phys. Rev. D **62**, 094503 (2000).
[5] S. R. Sharpe and N. Shoresh, Phys. Rev. D **64**, 114510 (2001).
[6] S. R. Sharpe and R. L. Singleton, Phys. Rev. D **58**, 074501 (1998).
[7] W. Lee and S. R. Sharpe, Phys. Rev. D **60**, 114503 (1999).
[8] R. G. Edwards *et al.*, Phys. Rev. Lett. **96**, 052001 (2006).
[9] A. Ali Khan *et al.* (QCDSF Collaboration), Phys. Rev. D **74**, 094508 (2006).
[10] S. R. Beane and M. Savage, Nucl. Phys. **A709**, 319 (2002).
[11] T. R. Hemmert, M. Procura, and W. Weise, Phys. Rev. D **68**, 075009 (2003).
[12] M. Procura, B. U. Musch, T. R. Hemmert, and W. Weise, Phys. Rev. D **75**, 014503 (2007).
[13] S. R. Beane and M. J. Savage, Phys. Rev. D **68**, 114502 (2003).
[14] F. J. Jiang, arXiv:hep-lat/0703012.

[15] S. R. Beane and M. J. Savage, Phys. Rev. D **70**, 074029 (2004).
[16] W. Detmold and M. J. Savage, Phys. Lett. B **599**, 32 (2004).
[17] B. Smigielski and J. Wasem, Phys. Rev. D **76**, 074503 (2007).
[18] E. Jenkins and A. V. Manohar, Phys. Lett. B **255**, 558 (1991).
[19] E. Jenkins and A. V. Manohar, Phys. Lett. B **259**, 353 (1991).
[20] E. Jenkins, Nucl. Phys. **B375**, 561 (1992).
[21] R. P. Springer, arXiv:hep-ph/9508324.
[22] M. J. Savage and J. Walden, Phys. Rev. D **55**, 5376 (1997).
[23] B. Borasoy and B. R. Holstein, Eur. Phys. J. C **6**, 85 (1999).
[24] A. Abd El-Hady, J. Tandean, and G. Valencia, Nucl. Phys. **A651**, 71 (1999).
[25] R. P. Springer, Phys. Lett. B **461**, 167 (1999).
[26] A. Abd El-Hady and J. Tandean, Phys. Rev. D **61**, 114014 (2000).
[27] S. R. Beane, P. F. Bedaque, A. Parreno, and M. J. Savage, Nucl. Phys. **A747**, 55 (2005).
[28] A. Gasparyan, J. Haidenbauer, C. Hanhart, and J. Speth, Phys. Rev. C **69**, 034006 (2004).
[29] F. Hinterberger and A. Sibirtsev, Eur. Phys. J. A **21**, 313 (2004).
[30] S. R. Beane *et al.*, Nucl. Phys. **A794**, 62 (2007).
[31] H.-W. Lin, arXiv:0707.3844.
[32] H.-W. Lin and K. Orginos, arXiv:0712.1214.
[33] W. Detmold and C. J. David Lin, Phys. Rev. D **71**, 054510 (2005).
[34] O. Bar, C. Bernard, G. Rupak, and N. Shoresh, Phys. Rev. D **72**, 054502 (2005).
[35] B. C. Tiburzi, Phys. Rev. D **72**, 094501 (2005).
[36] J. W. Chen, D. O'Connell, and A. Walker-Loud, arXiv:0706.0035.
[37] J. N. Labrenz and S. R. Sharpe, Phys. Rev. D **54**, 4595 (1996).
[38] M. J. Savage, Nucl. Phys. **A700**, 359 (2002).
[39] J.-W. Chen and M. J. Savage, Phys. Rev. D **65**, 094001 (2002).
[40] V. Bernard, H. W. Fearing, T. R. Hemmert, and U. G. Meissner, Nucl. Phys. **A635**, 121 (1998); **A642**, 563(E) (1998).
[41] B. Borasoy, Phys. Rev. D **59**, 054021 (1999).
[42] M. Kim and S. Kim, Phys. Rev. D **58**, 074509 (1998).
[43] J. Kambor and M. Mojzis, J. High Energy Phys. 04 (1999) 031.
[44] W. Detmold, W. Melnitchouk, and A. W. Thomas, Phys. Rev. D **66**, 054501 (2002).
[45] S.-L. Zhu, S. Puglia, and M. J. Ramsey-Musolf, Phys. Rev. D **63**, 034002 (2001); **63**, 034014 (2001).
[46] V. Bernard and Ulf-G. Meissner, Phys. Lett. B **639**, 278 (2006).
[47] B. C. Tiburzi, Phys. Rev. D **71**, 054504 (2005).
[48] B. C. Tiburzi, Phys. Lett. B **617**, 40 (2005).
[49] S. L. Adler and Y. Dothan, Phys. Rev. **151**, 1267 (1966).